ELSEVIER

International Journal of Solids and Structures 41 (2004) 3771–3791

INTERNATIONAL JOURNAL OF SOLIDS and STRUCTURES

www.elsevier.com/locate/ijsolstr

Internal symmetry groups for the Drucker–Prager material model of plasticity and numerical integrating methods

Chein-Shan Liu *

Department of Mechanical and Mechatronic Engineering, National Taiwan Ocean University, Keelung 20224, Taiwan, ROC

Received 3 November 2003; received in revised form 12 February 2004
Available online 19 March 2004

Abstract

Internal symmetries for the Drucker–Prager material model and numerical methods based on them are investigated here. We first convert the non-linear constitutive equations to a Lie type system $\dot{\mathbf{X}} = \mathbf{A}(\mathbf{X}, t)\mathbf{X}$, where $\mathbf{A} \in sl(5, 2, \mathbb{R})$ is a Lie algebra of the special orthochronous pseudo-linear group $SL(5, 2, \mathbb{R})$. The underlying space of Drucker–Prager model in the plastic phase is a pseudo-sphere in the pseudo-Riemann manifold, which is locally a pseudo-Euclidean space $\mathbb{E}^7_{5,2}$, and whose metric tensor is indefinite having signature (5,2) and also depends on the temporal component. Then, we split the Drucker–Prager yield condition into two "sub-yield" conditions, which together with two integrating factors idea led us to derive two Lie type systems in the product space $\mathbb{M}^{5+1} \otimes \mathbb{M}^{1+1}$. The Lie algebra is the direct sum $so(5, 1) \oplus so(1, 1)$, and the symmetry group is thus $SO_o(5, 1) \otimes SO_o(1, 1)$. These results are essential from computational aspect. Based on these symmetry groups exponential mappings are developed, which update stress points exactly on the yield surface at every time increment without any iteration. As an example, the results calculated by using the two different group preserving schemes are compared to that calculated by the Runge–Kutta scheme together with the Newton–Raphson iterative solution of a non-linear algebraic equation which enforcing the consistency condition.

Keywords: Elastoplasticity; Drucker–Prager model; Pseudo-Riemann manifold; Internal symmetry; Consistent scheme

1. Introduction

Due to its extreme versatility and accuracy in modeling material behavior, plasticity theory has gained widespread use in numerical simulations of practical geotechnical engineering problems. A wide range of geotechnical materials including rock, concrete, soil and porous metals display pressure-dependent plastic yielding behavior and inelastic volumetric dilatancy. Building upon the pioneering works of Drucker and Prager (1952) on soil plasticity, the modern trend has been toward the development of more and more elaborate and complicated elastoplastic constitutive models which resemble the behavior of geomaterials more closely. Also, considerable efforts were devoted to the study of deformation fields and crack growth

* Tel.: +886-2-2462-2192x3252; fax: +886-2-2462-0836.
E-mail address: csliu@mail.ntou.edu.tw (C.-S. Liu).

0020-7683/$ - see front matter © 2004 Elsevier Ltd. All rights reserved.
doi:10.1016/j.ijsolstr.2004.02.035

characteristics in pressure-sensitive materials, for example, Li and Pan (1990); Miao and Drugan (1993); Borja (2000); Wells and Sluys (2001); Bousshine et al. (2001); Borja and Regueiro (2001), and references therein.

The numerical solution of elastoplastic boundary-value problems in solid mechanics is based on an iterative solution of the discretized momentum balance equations. Typically, for every loading time step with a converged configuration at step ℓ, solution involves the following steps (Simo and Hughes, 1998): (1) The discretized momentum equations are used to compute a new configuration for step $\ell+1$ via an incremental motion which is used to compute at every stress point incremental strains $\Delta\boldsymbol{\varepsilon}$. (2) At every stress point, for the given incremental strains $\Delta\boldsymbol{\varepsilon}$, new values of state variables $\boldsymbol{\sigma}(\ell+1)$ are obtained by integration of the local constitutive equations. (3) From the new computed stresses, balance of momentum is checked and if violated iterations are performed by returning to step (1).

For most computational architectures currently in use, steps (1) and (3) are carried out by finite-element/finite-difference procedures. In this paper attention is focused on step (2) for the elastoplastic constitutive equations with the Drucker–Prager yielding criterion and associated plastic flow rule. This step is a central problem in computational plasticity as it corresponds to the main role played by the constitutive equations. However, due to non-linear nature of the model equations in plasticity, the difficulties for developing exact method to solve them are involved in this issue. For its great consumption of computational time, and the efficiency and accuracy of the calculations of mechanical problems being strongly influenced by the efficiency and accuracy of constitutive-equations solving schemes, it has drawn much attention over the past several decades and has stimulated many researches in this issue to develop accurate and economic algorithms; see, for example, Nagtegaal et al. (1974); Hughes (1984); Ortiz and Popov (1985); Simo and Taylor (1985); Loret and Prevost (1986); Hong and Liou (1993); Simo and Hughes (1998); Hong and Liu (1999a, 2000); Büttner and Simeon (2002); Auricchio and Beirão da Veiga, 2003; Hjiaj et al. (2003); Mukherjee and Liu (2003) and Liu (2001a, 2004a,b) among many others.

A numerical scheme which preserves symmetry and utilizes the invariance property from one time step to the next one or few steps will be more capable of capturing key features during elastoplastic deformation and have long-term stability and much improved efficiency and accuracy. Therefore the issue of internal symmetries in the constitutive laws of plasticity is not only important in its own right, but will also find applications to the computational plasticity.

It deserves to noting recent attempt to present a unified theoretically and computationally convenient treatment of the backward-difference scheme for the integration of complex constitutive models; see, e.g., Cocchetti and Perego (2003). On the other hand, some recent attempts to propose the integration schemes based on the internal symmetries of simple elastoplastic constitutive models also deserve a further attention. A novel formulation for elastoplasticity has been recently developed by Hong and Liu (1999a,b, 2000); Liu and Hong (2001); Mukherjee and Liu (2003), and Liu (2001a, 2004a,b). These authors have explored the internal symmetry groups of the constitutive models for perfect elastoplasticity with or without considering large deformation, for bilinear elastoplasticity, for visco-elastoplasticity, for isotropic work-hardening elastoplasticity, as well as for mixed-hardening elastoplasticity to ensure that the plastic consistency condition is exactly satisfied at each time step once the computational schemes can take these symmetries into account.

The symmetry groups for these simple models are either Lorentz group or Poincaré group, and the underlying spaces are all flat Minkowski spacetime. The models considered were all restricted to pressure independent. However, it is interesting to observe the symmetry groups of the models that take the pressure effect into account. In this paper we consider a constitutive model of Drucker–Prager type (in Sections 2 and 3) and manage to put it in a more appropriate setting (in Sections 4 and 5) such that the internal spacetime structure and the internal symmetries (Sections 6 and 7) of the model are brought out. Using the internal symmetry inherent in the constitutive model we develop a consistent scheme based on one-integrating factor formulation (in Section 8). We also develop another one consistent scheme based on two-

integrating factors formulation (in Section 9), and then a Runge–Kutta numerical scheme with a Newton–Raphson iterative solution of an algebraic equation to enforce the consistency condition (in Section 10). One direct benefit of our new schemes is that the stress point is automatically updated on the yield surface without iterative calculations for every time step. This is what the conventional constitutive numerical schemes desired and failed to achieve. Finally, we draw some conclusions (in Section 11).

2. The model

The small-strain elastoplastic model equipped with the yield criterion of Drucker and Prager (1952) can be reformulated as follows:

$$\dot{\boldsymbol{\varepsilon}} = \dot{\boldsymbol{\varepsilon}}^e + \dot{\boldsymbol{\varepsilon}}^p, \tag{1}$$

$$\dot{\boldsymbol{\sigma}} = 2G\dot{\boldsymbol{\varepsilon}}^e + \frac{3K-2G}{3}(\mathrm{tr}\,\dot{\boldsymbol{\varepsilon}}^e)\mathbf{I}_3, \tag{2}$$

$$\dot{\lambda}\frac{\partial f}{\partial \boldsymbol{\sigma}} = 2\tau_y\dot{\boldsymbol{\varepsilon}}^p, \tag{3}$$

$$f \leqslant 0, \tag{4}$$

$$\dot{\lambda} \geqslant 0, \tag{5}$$

$$\dot{\lambda} f = 0, \tag{6}$$

where a superimposed dot represents the material time derivative, $\mathbf{I}_k$ is the second order identity tensor with dimensions k, and the symbol tr denotes the trace of the tensor. The yield function is

$$f := \frac{1}{2}\mathbf{s}\cdot\mathbf{s} - (\tau_y - \alpha\mathrm{tr}\,\boldsymbol{\sigma})^2, \tag{7}$$

where

$$\mathbf{s} := \boldsymbol{\sigma} - \frac{1}{3}(\mathrm{tr}\,\boldsymbol{\sigma})\mathbf{I}_3 \tag{8}$$

is stress deviator, and a dot between two same order tensors denotes their Euclidean inner product. Here we assume $\tau_y - \alpha\mathrm{tr}\,\boldsymbol{\sigma} > 0$, such that the original yield condition $\sqrt{\mathbf{s}\cdot\mathbf{s}/2} + \alpha\mathrm{tr}\,\boldsymbol{\sigma} = \tau_y$ proposed by Drucker and Prager is recovered. The stress admissible region is the interior of the cone as shown in Fig. 1.

The model needs only four experimentally determined material constants, namely the bulk modulus K, the shear modulus G, the shear yield strength τ_y, and the frictional coefficient α, which are postulated to be

$$\frac{1}{K} \geqslant 0, \quad G > 0, \quad \tau_y > 0, \quad \alpha \geqslant 0. \tag{9}$$

The two material constants τ_y and α may be related to the cohesion stress c and internal friction angle ϕ through the following relations:

$$\tau_y = \frac{3c}{\sqrt{9+12\tan^2\phi}}, \quad \alpha = \frac{\tan\phi}{\sqrt{9+12\tan^2\phi}}. \tag{10}$$

Such that the Drucker–Prager cone is the inner tangent cone to the Mohr–Coulomb pyramid; see, for example, Bousshine et al. (2001).

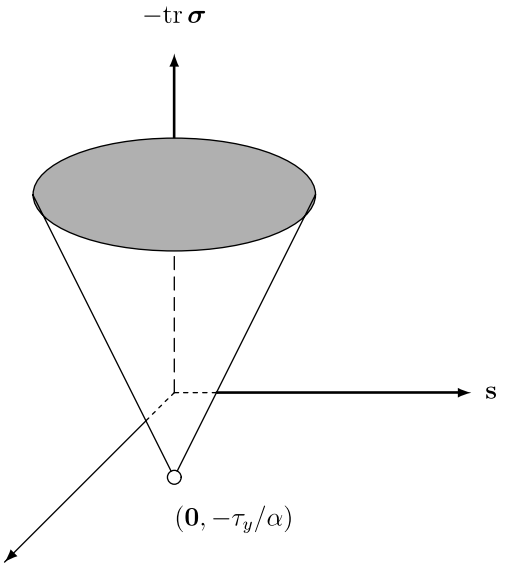

Fig. 1. The yield cone of the Drucker–Prager model. The vertex point $(\mathbf{0}, -\tau_y/\alpha)$ of the cone in the coordinates $(\mathbf{s}, -\mathrm{tr}\,\boldsymbol{\sigma})$ is deleted.

Taking the traces of both sides of Eq. (3) one has

$$\mathrm{tr}\,\dot{\boldsymbol{\varepsilon}}^p = \frac{3\alpha\dot{\lambda}}{\tau_y}(\tau_y - \alpha\,\mathrm{tr}\,\boldsymbol{\sigma}), \tag{11}$$

that is, the model implies plastic compressibility. It shows that plastic deformation must be accompanied by an increase in volume if $\alpha > 0$, which is known as material dilatancy.

3. The switch of plastic irreversibility

From Eqs. (1)–(3) and (7) it follows that

$$\mathrm{tr}\,\dot{\boldsymbol{\sigma}} = 3K\,\mathrm{tr}\,\dot{\boldsymbol{\varepsilon}} - \frac{9K\alpha}{\tau_y}\dot{\lambda}(\tau_y - \alpha\,\mathrm{tr}\,\boldsymbol{\sigma}), \tag{12}$$

$$\dot{\mathbf{s}} = 2G\dot{\mathbf{e}} - \frac{\dot{\lambda}}{\gamma_y}\mathbf{s}, \tag{13}$$

where

$$\gamma_y := \frac{\tau_y}{G} > 0 \tag{14}$$

is a material constant and

$$\dot{\mathbf{e}} := \dot{\boldsymbol{\varepsilon}} - \frac{1}{3}(\mathrm{tr}\,\dot{\boldsymbol{\varepsilon}})\mathbf{I}_3 \tag{15}$$

is strain rate deviator.

Substituting Eqs. (12) and (13) into the consistency condition $\dot{f}=0$ yields

$$\left[\frac{1}{\gamma_y}\mathbf{s}\cdot\mathbf{s}+\frac{18K\alpha^2}{\tau_y}(\tau_y-\alpha\mathrm{tr}\boldsymbol{\sigma})^2\right]\dot{\lambda}=2G\mathbf{s}\cdot\dot{\mathbf{e}}+6K\alpha(\tau_y-\alpha\mathrm{tr}\boldsymbol{\sigma})\mathrm{tr}\dot{\boldsymbol{\varepsilon}}.$$

Because of

$$\frac{1}{\gamma_y}\mathbf{s}\cdot\mathbf{s}+\frac{18K\alpha^2}{\tau_y}(\tau_y-\alpha\mathrm{tr}\boldsymbol{\sigma})^2>0,$$

we have

$$f=0\Rightarrow G\mathbf{s}\cdot\dot{\mathbf{e}}+3K\alpha(\tau_y-\alpha\mathrm{tr}\boldsymbol{\sigma})\mathrm{tr}\dot{\boldsymbol{\varepsilon}}>0\Longleftrightarrow\dot{\lambda}>0, \tag{16}$$

from which the following statement can be deduced:

$$\{f=0\text{ and }G\mathbf{s}\cdot\dot{\mathbf{e}}+3K\alpha(\tau_y-\alpha\mathrm{tr}\boldsymbol{\sigma})\mathrm{tr}\dot{\boldsymbol{\varepsilon}}>0\}\Rightarrow\dot{\lambda}>0. \tag{17}$$

On the other hand, if $\dot{\lambda}>0$, Eq. (6) ensures $f=0$, which together with Eq. (16) lead to

$$\dot{\lambda}>0\Rightarrow\{f=0\text{ and }G\mathbf{s}\cdot\dot{\mathbf{e}}+3K\alpha(\tau_y-\alpha\mathrm{tr}\boldsymbol{\sigma})\mathrm{tr}\dot{\boldsymbol{\varepsilon}}>0\}. \tag{18}$$

From Eqs. (17) and (18) we thus conclude that the yield condition $f=0$ and the straining condition $G\mathbf{s}\cdot\dot{\mathbf{e}}+3K\alpha(\tau_y-\alpha\mathrm{tr}\boldsymbol{\sigma})\mathrm{tr}\dot{\boldsymbol{\varepsilon}}>0$ are sufficient and necessary for plastic irreversibility $\dot{\lambda}>0$. Considering this and the inequality (5), we thus reveal the following criteria for plastic irreversibility:

$$\dot{\lambda}=\frac{\tau_y[G\mathbf{s}\cdot\dot{\mathbf{e}}+3K\alpha(\tau_y-\alpha\mathrm{tr}\boldsymbol{\sigma})\mathrm{tr}\dot{\boldsymbol{\varepsilon}}]}{R(\tau_y-\alpha\mathrm{tr}\boldsymbol{\sigma})^2}>0\quad\text{if }f=0\quad\text{and}\quad G\mathbf{s}\cdot\dot{\mathbf{e}}+3K\alpha(\tau_y-\alpha\mathrm{tr}\boldsymbol{\sigma})\mathrm{tr}\dot{\boldsymbol{\varepsilon}}>0, \tag{19}$$

$$\dot{\lambda}=0\quad\text{if }f<0\quad\text{or}\quad G\mathbf{s}\cdot\dot{\mathbf{e}}+3K\alpha(\tau_y-\alpha\mathrm{tr}\boldsymbol{\sigma})\mathrm{tr}\dot{\boldsymbol{\varepsilon}}\leqslant 0, \tag{20}$$

where

$$R:=G+9K\alpha^2 \tag{21}$$

is a material constant.

According to the complementary trios (4)–(6), there are just two phases: (i) $\dot{\lambda}>0$ and $f=0$, and (ii) $\dot{\lambda}=0$ and $f\leqslant 0$. From the criterion (19) it is clear that (i) corresponds to the plastic phase (or called the on-phase, or the elastoplastic phase) while (ii) to the elastic phase (or called the off-phase). During the plastic phase, $\dot{\lambda}>0$, the mechanism of plasticity is on, the mechanical process is irreversible, and the material exhibits elastoplastic behavior, while in the elastic phase, $\dot{\lambda}=0$, the mechanism of plasticity is off, the mechanical process is reversible, and the material responds elastically. Thus Eqs. (19) and (20) are called the on–off switching criteria for the on–off switch of the mechanism of plasticity. Substituting Eq. (19) for $\dot{\lambda}$ into Eqs. (12) and (13) results in a coupled highly non-linear differential equations system for $\mathrm{tr}\boldsymbol{\sigma}$ and $\mathbf{s}$. In the following we are going to reduce these non-linearities through a group-theoretic approach.

4. An eight-dimensional Lie algebra representation

In this section and the next one we will manage to put the constitutive model in such a form as to reveal internal symmetry. We first rearrange Eq. (12) into

$$\frac{\mathrm{d}}{\mathrm{d}t}[\exp(-a_0\lambda)(\tau_y-\alpha\mathrm{tr}\boldsymbol{\sigma})]+\frac{\dot{\lambda}}{\gamma_y}[\exp(-a_0\lambda)(\tau_y-\alpha\mathrm{tr}\boldsymbol{\sigma})]=\frac{(\eta-1)G\alpha}{\eta\exp(a_0\lambda)}\mathrm{tr}\dot{\boldsymbol{\varepsilon}}, \tag{22}$$

where

$$a_0 := \frac{3(1-\eta)\alpha^2+\eta}{\eta\gamma_y} \tag{23}$$

is a material constant, and

$$\eta := \frac{1-2\nu}{3}, \quad 0 \leqslant \eta < 1, \tag{24}$$

is called the index of compressibility. Through the above arrangement Eqs. (22) and (13) thus possess the same integrating factor X^0 defined by

$$X^0 := \exp\frac{\lambda}{\gamma_y}. \tag{25}$$

Then, by noting that

$$\exp(a_0\lambda) = (X^0)^{b_0}, \tag{26}$$

where

$$b_0 := a_0\gamma_y = \frac{3(1-\eta)\alpha^2+\eta}{\eta}, \tag{27}$$

Eq. (22) can be written as

$$\frac{\mathrm{d}}{\mathrm{d}t}[(X^0)^{1-b_0}(\tau_y - \alpha\mathrm{tr}\boldsymbol{\sigma})] = \frac{(\eta-1)G\alpha}{\eta(X^0)^{b_0-1}}\mathrm{tr}\dot{\boldsymbol{\varepsilon}}. \tag{28}$$

Simultaneously, Eq. (13) changes to

$$\frac{\mathrm{d}}{\mathrm{d}t}(X^0\mathbf{s}) = 2GX^0\dot{\mathbf{e}}. \tag{29}$$

Let us introduce

$$\widetilde{\mathbf{X}} = \begin{bmatrix}\widetilde{\mathbf{X}}^s \\ X^0\end{bmatrix} = \begin{bmatrix}\widetilde{X}^1 \\ \vdots \\ \widetilde{X}^7 \\ X^0\end{bmatrix} := \frac{X^0}{\tau_y}\begin{bmatrix} \frac{s^{11}}{\sqrt{2}} \\ \frac{s^{22}}{\sqrt{2}} \\ \frac{s^{33}}{\sqrt{2}} \\ s^{23} \\ s^{13} \\ s^{12} \\ (X^0)^{-b_0}(\tau_y - \alpha\mathrm{tr}\boldsymbol{\sigma}) \\ \tau_y \end{bmatrix}. \tag{30}$$

The yield condition

$$f = \frac{1}{2}\mathbf{s}\cdot\mathbf{s} - (\tau_y - \alpha\mathrm{tr}\boldsymbol{\sigma})^2 = 0$$

thus can be expressed as

$$\frac{\tau_y^2}{(X^0)^2}\left[\sum_{i=1}^{6}(\widetilde{X}^i)^2 - (X^0)^{2b_0}(\widetilde{X}^7)^2\right] = 0.$$

Since $\tau_y > 0$, the above equation can be rearranged to

$$\frac{1}{(X^0)^2}\left[\sum_{i=1}^{6}(\widetilde{X}^i)^2 - (X^0)^{2b_0}(\widetilde{X}^7)^2 - (X^0)^2\right] = -1.$$

In terms of $\tilde{\mathbf{g}}$ defined by

$$\tilde{\mathbf{g}} = \frac{1}{(X^0)^2}\begin{bmatrix} \mathbf{I}_6 & \mathbf{0}_{6\times1} & \mathbf{0}_{6\times1} \\ \mathbf{0}_{1\times6} & -(X^0)^{2b_0} & 0 \\ \mathbf{0}_{1\times6} & 0 & -1 \end{bmatrix}, \tag{31}$$

we obtain

$$\widetilde{\mathbf{X}}^{\mathrm{T}}\tilde{\mathbf{g}}\widetilde{\mathbf{X}} = -1. \tag{32}$$

It is an equivalent form of the Drucker–Prager yield condition in the space of $\widetilde{\mathbf{X}}$. The space endows such a metric tensor $\tilde{\mathbf{g}}$ with signature (6,2) is known as a pseudo-Riemann manifold, which is locally a pseudo-Euclidean space denoted by $\mathbb{E}^8_{6,2}$; and the above equation signifies a pseudo-sphere in such a space. The above superscript T denotes the transpose.

Furthermore, Eqs. (29) and (28) together become

$$\frac{\mathrm{d}}{\mathrm{d}t}\widetilde{\mathbf{X}}^s = \widetilde{\mathbf{A}}^s_0 X^0, \tag{33}$$

where

$$\widetilde{\mathbf{A}}^s_0 := \frac{2}{\gamma_y}\left[\frac{\dot{e}_{11}}{\sqrt{2}} \quad \frac{\dot{e}_{22}}{\sqrt{2}} \quad \frac{\dot{e}_{33}}{\sqrt{2}} \quad \dot{e}_{23} \quad \dot{e}_{13} \quad \dot{e}_{12} \quad \frac{(\eta-1)\alpha}{2\eta(X^0)^{b_0}}\operatorname{tr}\dot{\boldsymbol{\varepsilon}}\right]^{\mathrm{T}}. \tag{34}$$

In view of Eqs. (19) and (32) the on–off switching criteria become

$$\dot{X}^0 = \widetilde{\mathbf{A}}^0_s\widetilde{X}^s \quad \text{if } \widetilde{\mathbf{X}}^{\mathrm{T}}\tilde{\mathbf{g}}\widetilde{\mathbf{X}} = -1 \quad \text{and} \quad \widetilde{\mathbf{A}}^0_s\widetilde{\mathbf{X}}^s > 0, \tag{35}$$

$$\dot{X}^0 = 0 \quad \text{if } \widetilde{\mathbf{X}}^{\mathrm{T}}\tilde{\mathbf{g}}\widetilde{\mathbf{X}} < -1 \quad \text{or} \quad \widetilde{\mathbf{A}}^0_s\widetilde{\mathbf{X}}^s \leqslant 0, \tag{36}$$

in which

$$\widetilde{\mathbf{A}}^0_s := \frac{2}{\gamma_y F_1}\left[\frac{\dot{e}_{11}}{\sqrt{2}} \quad \frac{\dot{e}_{22}}{\sqrt{2}} \quad \frac{\dot{e}_{33}}{\sqrt{2}} \quad \dot{e}_{23} \quad \dot{e}_{13} \quad \dot{e}_{12} \quad \frac{(1-\eta)\alpha(X^0)^{b_0}}{2\eta}\operatorname{tr}\dot{\boldsymbol{\varepsilon}}\right], \tag{37}$$

$$F_1 := \frac{R}{G}(X^0)^{(2b_0-2)}(\widetilde{X}^7)^2. \tag{38}$$

Note that $\widetilde{\mathbf{A}}^s_0$ is a seven-dimensional column vector; conversely, $\widetilde{\mathbf{A}}^0_s$ is a seven-dimensional row vector.

Organizing Eqs. (33), (35) and (36) we have

$$\frac{\mathrm{d}}{\mathrm{d}t}\widetilde{\mathbf{X}} = \widetilde{\mathbf{A}}\widetilde{\mathbf{X}}, \tag{39}$$

where

$$\widetilde{\mathbf{A}} = \begin{bmatrix} \mathbf{0}_{7\times7} & \widetilde{\mathbf{A}}^s_0 \\ \widetilde{\mathbf{A}}^0_s & 0 \end{bmatrix} \text{ if } \widetilde{\mathbf{X}}^{\mathrm{T}}\tilde{\mathbf{g}}\widetilde{\mathbf{X}} = -1 \quad \text{and} \quad \widetilde{\mathbf{A}}^0_s\widetilde{\mathbf{X}}^s > 0, \tag{40}$$

$$\widetilde{\mathbf{A}} = \begin{bmatrix} \mathbf{0}_{7\times7} & \widetilde{\mathbf{A}}^s_0 \\ \mathbf{0}_{1\times7} & 0 \end{bmatrix} \text{ if } \widetilde{\mathbf{X}}^{\mathrm{T}}\tilde{\mathbf{g}}\widetilde{\mathbf{X}} < -1 \quad \text{or} \quad \widetilde{\mathbf{A}}^0_s\widetilde{\mathbf{X}}^s \leqslant 0. \tag{41}$$

Eq. (39) is an eight-dimensional Lie algebra representation of the constitutive model (1)–(6). Because it is easy to check that

$$\operatorname{tr}\widetilde{\mathbf{A}} = 0, \tag{42}$$

$\widetilde{\mathbf{A}}$ in the plastic phase is a Lie algebra of $sl(6,2,\mathbb{R})$, which depends on $\widetilde{\mathbf{X}}$, and thus Eq. (39) is not a linear system.

5. A seven-dimensional Lie algebra representation

Due to the vanishing traces of the deviatoric tensors $\mathbf{s}$ and $\dot{\mathbf{e}}$, the third components in Eqs. (30) and (39) can be obtained from the first two components:

$$s^{33} = -s^{11} - s^{22}, \quad \dot{e}_{33} = -\dot{e}_{11} - \dot{e}_{22}. \tag{43}$$

To delete this redundancy, let us introduce

$$\mathbf{X} = \begin{bmatrix} \mathbf{X}^s \\ X^0 \end{bmatrix} = \begin{bmatrix} X^1 \\ \cdot \\ \cdot \\ \cdot \\ \cdot \\ X^6 \\ X^0 \end{bmatrix} := \frac{X^0}{\tau_y} \begin{bmatrix} a_1 s^{11} + a_2 s^{22} \\ a_3 s^{11} + a_4 s^{22} \\ s^{23} \\ s^{13} \\ s^{12} \\ (X^0)^{-b_0}(\tau_y - \alpha \operatorname{tr}\boldsymbol{\sigma}) \\ \tau_y \end{bmatrix}, \tag{44}$$

where

$$a_1 := \sin\left(\theta + \frac{\pi}{3}\right), \quad a_2 := \sin\theta, \quad a_3 := \cos\left(\theta + \frac{\pi}{3}\right), \quad a_4 := \cos\theta, \tag{45}$$

with θ being any real number. The on–off switching criteria turn out to be

$$\dot{X}^0 = \mathbf{A}_s^0 \mathbf{X}^s \quad \text{if } \mathbf{X}^{\mathrm{T}}\mathbf{g}\mathbf{X} = -1 \quad \text{and} \quad \mathbf{A}_s^0 \mathbf{X}^s > 0, \tag{46}$$

$$\dot{X}^0 = 0 \quad \text{if } \mathbf{X}^{\mathrm{T}}\mathbf{g}\mathbf{X} < -1 \quad \text{or} \quad \mathbf{A}_s^0 \mathbf{X}^s \leqslant 0, \tag{47}$$

where

$$\mathbf{g} := \frac{1}{(X^0)^2} \begin{bmatrix} \mathbf{I}_5 & \mathbf{0}_{5\times 1} & \mathbf{0}_{5\times 1} \\ \mathbf{0}_{1\times 5} & -(X^0)^{2b_0} & 0 \\ \mathbf{0}_{1\times 5} & 0 & -1 \end{bmatrix}, \tag{48}$$

$$\begin{aligned} \mathbf{A}_s^0 &= \begin{bmatrix} A_1^0 & A_2^0 & A_3^0 & A_4^0 & A_5^0 & A_6^0 \end{bmatrix} \\ &:= \frac{2}{\gamma_y F_2} \left[a_1\dot{e}_{11} + a_2\dot{e}_{22} \quad a_3\dot{e}_{11} + a_4\dot{e}_{22} \quad \dot{e}_{23} \quad \dot{e}_{13} \quad \dot{e}_{12} \quad \frac{(1-\eta)\alpha(X^0)^{b_0}}{2\eta} \operatorname{tr}\dot{\boldsymbol{\varepsilon}} \right], \end{aligned} \tag{49}$$

in which the factor F_2 becomes

$$F_2 := \frac{R}{G}(X^0)^{(2b_0-2)}(X^6)^2. \tag{50}$$

Thus, Eq. (39) is reduced to

$$\dot{\mathbf{X}} = \mathbf{A}\mathbf{X}, \tag{51}$$

where

$$\mathbf{A} = \begin{bmatrix} \mathbf{0}_{6\times 6} & \mathbf{A}_0^s \\ \mathbf{A}_s^0 & 0 \end{bmatrix} \quad \text{if } \mathbf{X}^{\mathrm{T}}\mathbf{g}\mathbf{X} = -1 \quad \text{and} \quad \mathbf{A}_s^0\mathbf{X}^s > 0, \tag{52}$$

$$\mathbf{A} = \begin{bmatrix} \mathbf{0}_{6\times 6} & \mathbf{A}_0^s \\ \mathbf{0}_{1\times 6} & 0 \end{bmatrix} \quad \text{if } \mathbf{X}^{\mathrm{T}}\mathbf{g}\mathbf{X} < -1 \quad \text{or} \quad \mathbf{A}_s^0\mathbf{X}^s \leqslant 0, \tag{53}$$

in which

$$\mathbf{A}_0^s = \begin{bmatrix} A_0^1 \\ A_0^2 \\ A_0^3 \\ A_0^4 \\ A_0^5 \\ A_0^6 \end{bmatrix} := \frac{2}{\gamma_y} \begin{bmatrix} a_1\dot{e}_{11} + a_2\dot{e}_{22} \\ a_3\dot{e}_{11} + a_4\dot{e}_{22} \\ \dot{e}_{23} \\ \dot{e}_{13} \\ \dot{e}_{12} \\ \frac{(\eta-1)\alpha}{2\eta(X^0)^{b_0}}\operatorname{tr}\dot{\boldsymbol{\varepsilon}} \end{bmatrix}. \tag{54}$$

Consequently, the underlying space of the Drucker–Prager model in the plastic phase is the following pseudo-sphere:

$$\mathbf{X}^{\mathrm{T}}\mathbf{g}\mathbf{X} = -1. \tag{55}$$

The space endows such a metric $\mathbf{g}$ with signature (5,2) and dependent on the temporal component X^0 as shown in Eq. (48) is known as a pseudo-Riemann manifold, which is locally a pseudo-Euclidean space denoted by $\mathbb{E}^7_{5,2}$. This is similar to the pseudo-Riemann spacetime structure for the mixed-hardening elastoplasticity as discussed by Liu (2003).

Note that Eq. (51) is a (5+2)-dimensional Lie algebra representation of the constitutive model (1)–(7), in which $\mathbf{X}$ and $\mathbf{A}$ are the augmented stress vector and the control tensor, respectively. The control tensor $\mathbf{A}$ organizes the input information of the strain rate tensor $\dot{\boldsymbol{\varepsilon}}$, and also depends on $\mathbf{X}$. Thus we obtain a Lie type equation

$$\dot{\mathbf{X}} = \mathbf{A}(\mathbf{X}, t)\mathbf{X}, \tag{56}$$

where the $\mathbf{A}$ of plastic phase satisfying

$$\operatorname{tr}\mathbf{A} = 0 \tag{57}$$

is a Lie algebra of $sl(5, 2, \mathbb{R})$.

6. *PSL*(5, 2, ℝ) symmetry in the plastic phase

Due to Eq. (51) we assert that the symmetry group of this model in the plastic phase is a one-parameter subgroup $\mathbf{G}(t)$ satisfying the following Lie type equation (see, e.g., Liu, 2001b):

$$\dot{\mathbf{G}}(t) = \mathbf{A}(\mathbf{G}(t), t)\mathbf{G}(t), \tag{58}$$

$$\mathbf{G}(0) = \mathbf{I}_7. \tag{59}$$

Thus the solution of Eq. (51) may be expressed in the following formula for the transition from the augmented stress $\mathbf{X}(t_1)$ at time t_1 to the augmented stress $\mathbf{X}(t)$ at time t:

$$\mathbf{X}(t) = [\mathbf{G}(t)\mathbf{G}^{-1}(t_1)]\mathbf{X}(t_1). \tag{60}$$

From Eqs. (5), (25) and (44) it follows that

$$X^0(t) \geqslant X^0(t') \geqslant X^0(t_i), \quad \forall\ t \geqslant t' \geqslant t_i, \tag{61}$$

which is applicable to both the on and off phases.

In the remainder of this section we concentrate on the plastic phase to bring out internal symmetry inherent in the model in the plastic phase. Denote by I_{on} an open, maximal, continuous time interval during which the mechanism of plasticity is on exclusively. From Eq. (52) it is easy to verify that the control tensor $\mathbf{A}$ in the plastic phase satisfies Eq. (57). Hence, the corresponding transformation $\mathbf{G}$ satisfies

$$\det \mathbf{G} = 1, \tag{62}$$

$$G_0^0 \geqslant 1. \tag{63}$$

Thereby the on-phase control tensor $\mathbf{A}$ is an element of the real Lie algebra $sl(5,2,\mathbb{R})$ and generates the on-phase transformation $\mathbf{G}$, which is thus an element of the special orthochronous pseudo-linear group $SL(5,2,\mathbb{R})$.

From Eq. (46), $\dot{X}^0 > 0$ strictly when the mechanism of plasticity is on; hence,

$$X^0(t) > X^0(t_1), \quad \forall\ t > t_1,\ \ t, t_1 \in I_{\text{on}}, \tag{64}$$

which means that in the sense of irreversibility there exists a future-pointing time-orientation from the augmented stress $\mathbf{X}(t_1)$ to $\mathbf{X}(t)$. Compare Eqs. (64) and (61). Moreover, such time-orientation is a causal one, because the augmented stress transition formula (60) and inequality (64) establish a causality relation between the two augmented stresses $\mathbf{X}(t_1)$ and $\mathbf{X}(t)$ in the sense that the preceding augmented stress $\mathbf{X}(t_1)$ influences the following augmented stress $\mathbf{X}(t)$ according to formula (60). Accordingly, the augmented stress $\mathbf{X}(t_1)$ chronologically and causally precedes the augmented stress $\mathbf{X}(t)$. This is indeed a common property for all models with inherent symmetry of the orthochronous group. By this symmetry a core connection among irreversibility, the time arrow of evolution, and causality has thus been established for plasticity in the plastic phase.

From Eq. (44) it follows that

$$\begin{bmatrix} s^{11} \\ s^{22} \\ s^{23} \\ s^{13} \\ s^{12} \\ \operatorname{tr}\boldsymbol{\sigma} \end{bmatrix} = \begin{bmatrix} a_4 & -a_2 & \mathbf{0}_{2\times 3} & \mathbf{0}_{2\times 1} \\ -a_3 & a_1 & & \\ \mathbf{0}_{3\times 2} & & \frac{\sqrt{3}}{2}\mathbf{I}_3 & \mathbf{0}_{3\times 1} \\ \mathbf{0}_{1\times 2} & & \mathbf{0}_{1\times 3} & \frac{-\sqrt{3}(X^0)^{b_0}}{2\alpha} \end{bmatrix} \frac{2\tau_y}{\sqrt{3}X^0}\mathbf{X}^s + \begin{bmatrix} 0 \\ 0 \\ 0 \\ 0 \\ 0 \\ \frac{\tau_y}{\alpha} \end{bmatrix}, \tag{65}$$

and one can determine the stress tensor $\boldsymbol{\sigma}(t)$ once the augmented stress vector $\mathbf{X}(t)$ is calculated. This is indeed a projective realization of the response. By this and the on-phase transition (60) one can map $\boldsymbol{\sigma}(t_1)$ to the current response $\boldsymbol{\sigma}(t)$.

7. $T(6)$ symmetry in the off-phase

Contrary to Eq. (60) of the plastic phase, the transition for the off phase is very simple. To find it, recall that Eqs. (58)–(60) are still applicable but with

$$\mathbf{G}(t) = \begin{bmatrix} \mathbf{I}_6 & \mathbf{T}(t) \\ \mathbf{0}_{1\times 6} & 1 \end{bmatrix}, \tag{66}$$

where $\mathbf{T}$ is of order 6×1 and governed by

$$\dot{\mathbf{T}} = \mathbf{A}_0^s,$$

in which $\mathbf{A}_0^s$ is given in Eq. (54) with X^0 fixed. Thus it is easy to show that $\mathbf{T} \in T(6)$, and $\mathbf{G} \in T(7)$; therefore, the constitutive law in the off-phase has an internal symmetry characterized by the translation group $T(6)$.

The inverse of Eq. (66) is given by

$$\mathbf{G}^{-1} = \begin{bmatrix} \mathbf{I}_6 & -\mathbf{T} \\ \mathbf{0}_{1\times 6} & 1 \end{bmatrix}. \tag{67}$$

Thus according to Eq. (60) we obtain

$$\begin{bmatrix} \mathbf{X}^s(t) \\ X^0(t) \end{bmatrix} = \begin{bmatrix} \mathbf{I}_6 & \mathbf{T}(t) - \mathbf{T}(t_1) \\ \mathbf{0}_{1\times 6} & 1 \end{bmatrix} \begin{bmatrix} \mathbf{X}^s(t_1) \\ X^0(t_1) \end{bmatrix}, \tag{68}$$

which is valid for the off-phase. In a similar way the stress response in the off-phase can be realized by invoking Eq. (65) and the off-phase transition formula (68).

In summary the stress response is the projective realization (65) of the on-phase transition formula (60) or the off-phase transition formula (68); switching between the two depends upon the control tensor $\mathbf{A}$ and obeys the on–off switching criteria (46) and (47). The switching from a transformation of the special orthochronous pseudo-linear group in the plastic phase to a translation transformation in the off-phase indicates that internal symmetry switches from one kind to another, and vice versa. As a result the constitutive model in the stress space of $\boldsymbol{\sigma}$ has symmetry switching between the translation group $T(6)$ acting on the admissible stresses in the interior of the cone as shown in Eqs. (4) and (7) as well as in Fig. 1, and the projective special orthochronous pseudo-linear group $PSL(5,2,\mathbb{R})$ acting on the yield hyper-surface.

8. Numerical method based on one-integrating factor formulation

For calculation purpose we may approximate the specified controlled-strain path by many rectilinear strain paths, such that $\dot{\boldsymbol{\varepsilon}}$ at each time step is constant, denoting by $\dot{\boldsymbol{\varepsilon}}(\ell)$ at a discrete time $t = t_\ell$. We first consider elastic phase. Under specified strain path $\dot{\boldsymbol{\varepsilon}}(\ell)$ and initial stress $\boldsymbol{\sigma}(\ell)$ the elastic response can be obtained by

$$\mathbf{s}(t) = \mathbf{s}(\ell) + 2G(t - t_\ell)\dot{\mathbf{e}}(\ell), \tag{69}$$

$$\operatorname{tr}\boldsymbol{\sigma}(t) = \operatorname{tr}\boldsymbol{\sigma}(\ell) + 3K(t - t_\ell)\operatorname{tr}\dot{\boldsymbol{\varepsilon}}(\ell). \tag{70}$$

The end time of elastic phase denoted by t_{on} can be determined according to the criterion (19) as follows. First solve for t the following algebraic equation

$$[\mathbf{s}(\ell) + (t - t_\ell)\dot{\mathbf{e}}(\ell)] \cdot [\mathbf{s}(\ell) + (t - t_\ell)\dot{\mathbf{e}}(\ell)] - 2[\tau_y - \alpha \operatorname{tr}\boldsymbol{\sigma}(\ell) - 3K\alpha(t - t_\ell)\operatorname{tr}\dot{\boldsymbol{\varepsilon}}(\ell)]^2 = 0, \tag{71}$$

which has been obtained by substituting the elastic equations (69) and (70) into the yield condition $\mathbf{s} \cdot \mathbf{s} - 2(\tau_y - \alpha \operatorname{tr}\boldsymbol{\sigma})^2 = 0$. However, the solution t of Eq. (71) must satisfy $G\mathbf{s}(t) \cdot \dot{\mathbf{e}}(\ell) + 3K\alpha[\tau_y - \alpha \operatorname{tr}\boldsymbol{\sigma}(t)]\operatorname{tr}\dot{\boldsymbol{\varepsilon}}(\ell) > 0$ in order to be a switch-on time t_{on}. If there exist no solutions to Eq. (71) or the solution t to Eq. (71) does not satisfy $G\mathbf{s}(t) \cdot \dot{\mathbf{e}}(\ell) + 3K\alpha[\tau_y - \alpha \operatorname{tr}\boldsymbol{\sigma}(t)]\operatorname{tr}\dot{\boldsymbol{\varepsilon}}(\ell) > 0$, then the strain path will not switch on the plastic mechanism.

From Eq. (71) we obtain a quadratic equation for $t - t_\ell$,

$$A(t - t_\ell)^2 + B(t - t_\ell) + C = 0,$$

where

$$A := 4G^2\dot{\mathbf{e}}(\ell)\cdot\dot{\mathbf{e}}(\ell) - 18K^2\alpha^2[\mathrm{tr}\,\dot{\boldsymbol{\varepsilon}}(\ell)]^2,$$
$$B := 4G\mathbf{s}(\ell)\cdot\dot{\mathbf{e}}(\ell) + 12K\alpha[\tau_y - \alpha\mathrm{tr}\,\boldsymbol{\sigma}(\ell)]\mathrm{tr}\,\dot{\boldsymbol{\varepsilon}}(\ell),$$
$$C := \mathbf{s}(\ell)\cdot\mathbf{s}(\ell) - 2[\tau_y - \alpha\mathrm{tr}\,\boldsymbol{\sigma}(\ell)]^2.$$

Thus, we have

$$t_{\mathrm{on}} = t_\ell + \frac{-B + \sqrt{B^2 - 4AC}}{2A}. \tag{72}$$

The evolutions of elastic equations are rather simple, and we below turn our attention to the numerical solutions of plastic equations. The numerical scheme would provide a medium to calculate the value of $\mathbf{X}$ at time $t = t_{\ell+1}$ when knowing $\mathbf{X}$ at time $t = t_\ell$. The evolution of $\mathbf{X}$ is governed by the dynamical law (51) with matrix $\mathbf{A}$ given by Eq. (52). Due to the piecewise linearity of controlled strain, $\dot{\boldsymbol{\varepsilon}}$ is constant in each time increment equal to Δt. Unluckily, due to the presence of X^0 and X^6 in Eqs. (49) and (54), this is not true for matrix $\mathbf{A}$. Therefore we approximate the solution of the dynamical law (51) by considering X^0 and X^6 constant in each single time step. Under such an additional hypothesis, the matrix $\mathbf{A}$ is constant, and so the numerical solution of Eq. (51) is found to be

$$\mathbf{X}(\ell+1) = \mathbf{G}(\ell)\mathbf{X}(\ell), \tag{73}$$

where

$$\mathbf{G}(\ell) := \exp[\Delta t\mathbf{A}(\ell)] = \begin{bmatrix} \mathbf{I}_6 + \frac{z_1-1}{\mathbf{A}_s^0(\ell)\mathbf{A}_0^s(\ell)}\mathbf{A}_0^s(\ell)\mathbf{A}_s^0(\ell) & \frac{z_2}{\sqrt{\mathbf{A}_s^0(\ell)\mathbf{A}_0^s(\ell)}}\mathbf{A}_0^s(\ell) \\ \frac{z_2}{\sqrt{\mathbf{A}_s^0(\ell)\mathbf{A}_0^s(\ell)}}\mathbf{A}_s^0(\ell) & z_1 \end{bmatrix}, \tag{74}$$

in which

$$z_1 := \cosh\left(\Delta t\sqrt{\mathbf{A}_s^0(\ell)\mathbf{A}_0^s(\ell)}\right), \quad z_2 := \sinh\left(\Delta t\sqrt{\mathbf{A}_s^0(\ell)\mathbf{A}_0^s(\ell)}\right). \tag{75}$$

In order to increase the accuracy we can adopt a second order group preserving scheme, which replaces $\mathbf{G}(\ell)$ in Eq. (73) by

$$\mathbf{G}(\bar{\ell}) := \exp[\Delta t\mathbf{A}(\bar{\ell})] = \begin{bmatrix} \mathbf{I}_6 + \frac{z_1-1}{\mathbf{A}_s^0(\bar{\ell})\mathbf{A}_0^s(\bar{\ell})}\mathbf{A}_0^s(\bar{\ell})\mathbf{A}_s^0(\bar{\ell}) & \frac{z_2}{\sqrt{\mathbf{A}_s^0(\bar{\ell})\mathbf{A}_0^s(\bar{\ell})}}\mathbf{A}_0^s(\bar{\ell}) \\ \frac{z_2}{\sqrt{\mathbf{A}_s^0(\bar{\ell})\mathbf{A}_0^s(\bar{\ell})}}\mathbf{A}_s^0(\bar{\ell}) & z_1 \end{bmatrix}, \tag{76}$$

where $\bar{\ell}$ denotes the value at time $t_\ell + \Delta t/2$ and

$$z_1 := \cosh\left(\Delta t\sqrt{\mathbf{A}_s^0(\bar{\ell})\mathbf{A}_0^s(\bar{\ell})}\right), \quad z_2 := \sinh\left(\Delta t\sqrt{\mathbf{A}_s^0(\bar{\ell})\mathbf{A}_0^s(\bar{\ell})}\right). \tag{77}$$

The value of $\mathbf{X}$ at time $t_\ell + \Delta t/2$ which appeared in $\mathbf{A}_s^0$ and $\mathbf{A}_0^s$ is calculated by

$$\mathbf{X}(\bar{\ell}) = \exp\left[\frac{\Delta t}{2}\mathbf{A}(\ell)\right]\mathbf{X}(\ell), \tag{78}$$

and then $\mathbf{X}(\ell+1)$ is calculated by

$$\mathbf{X}(\ell+1) = \mathbf{G}(\bar{\ell})\mathbf{X}(\ell) \tag{79}$$

with $\mathbf{G}(\bar{\ell})$ from Eq. (76).

To match the consistency condition exactly, we impose the condition (55) on the numerical solutions of $\mathbf{X}(\ell+1)$, which by Eq. (48) leads to

$$X^0(\ell+1)=\left(\frac{\sum_{i=1}^{5}(X^i(\ell+1))^2}{(X^6(\ell+1))^2}\right)^{1/(2b_0)}, \tag{80}$$

where $X^1(\ell+1),\ldots,X^6(\ell+1)$ are calculated by Eq. (79). Substituting $X^1(\ell+1),\ldots,X^6(\ell+1)$ and $X^0(\ell+1)$ into Eq. (65) we obtain $\mathbf{s}(\ell+1)$ and $\mathrm{tr}\boldsymbol{\sigma}(\ell+1)$ at the current step.

Now, let us apply the above scheme to a certain example. The material constants used in the calculations were $G=3000$ psi ≈ 20.67 MPa, $c=30$ psi ≈ 206.7 kPa, $\phi=40^\circ$ and $v=0.3$, and thus $\tau_y=21.55$ psi ≈ 148.48 kPa and $\alpha\approx 0.2$. Fig. 2 displays the stress strain curves under cyclically increasing amplitudes of deviatoric strains and a constant volumetric strain increment. The volumetric stress as shown in Fig. 2(f) is tending to large negative value due to dilatancy. It should note that the increasing of deviatoric stresses is not due to the hardening effect (which we not consider here) but is due to the dilatancy of volumetric strain.

In Fig. 3 we show the consistency error defined by $\mathbf{s}\cdot\mathbf{s}/2-(\tau_y-\alpha\mathrm{tr}\boldsymbol{\sigma})^2$. When this quantity is zero for all plastic loading time we obtain a consistent scheme which preserves the consistency condition. As shown in Fig. 3 the consistency error by the one-integrating factor scheme is zero.

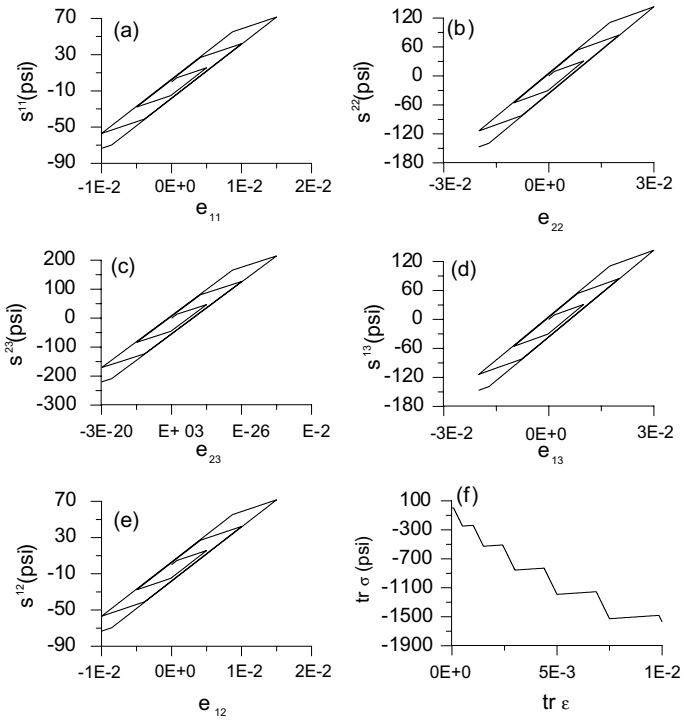

Fig. 2. The responses of the Drucker–Prager model under cyclically increasing amplitudes of deviatoric strains and a constant volumetric strain increment.

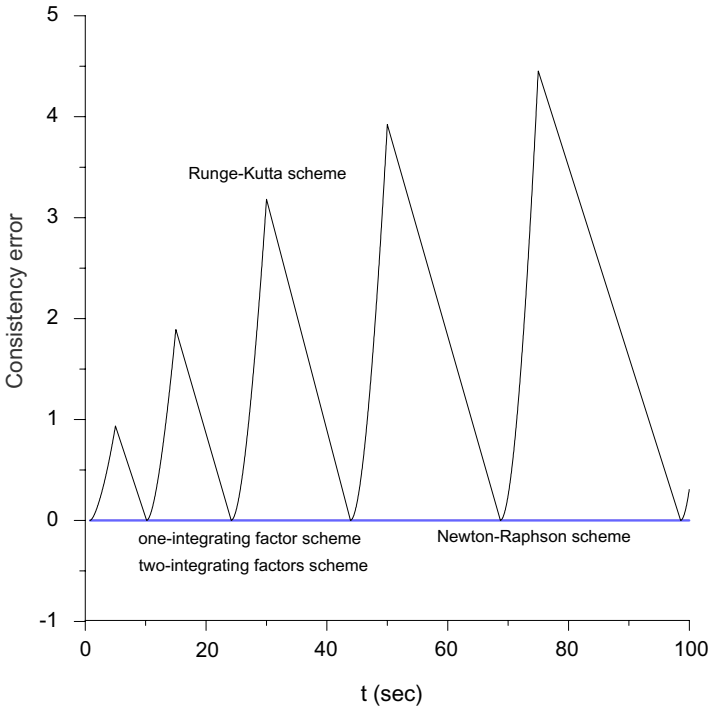

Fig. 3. The errors of consistency for different numerical schemes.

9. Numerical method based on two-integrating factors formulation

Now we turn our attention to a direct numerical solution of Eqs. (12) and (13). In terms of the integrating factor X^0 defined by Eq. (25), Eq. (13) can be written as

$$\frac{\mathrm{d}}{\mathrm{d}t}(X^0\mathbf{s}) = 2GX^0\dot{\mathbf{e}}. \tag{81}$$

Let $a(t) > 0$ and $b(t) > 0$ be unknown functions, such that

$$2a^2 = \mathbf{s}\cdot\mathbf{s}, \quad b^2 = (\tau_y - \alpha \mathrm{tr}\boldsymbol{\sigma})^2, \quad a^2 - b^2 = 0, \tag{82}$$

the last of which is due to the yield condition. Taking the inner product of Eq. (81) with $\mathbf{s}$ and noting $\mathbf{s}\cdot\mathbf{s} = 2a^2$ and $\mathbf{s}\cdot\dot{\mathbf{s}} = 2a\dot{a}$, we obtain

$$\frac{\mathrm{d}}{\mathrm{d}t}(aX^0) = GX^0a^{-1}\mathbf{s}\cdot\dot{\mathbf{e}}. \tag{83}$$

As before, we let

$$\mathbf{X}_a = \begin{bmatrix} \mathbf{X}_a^s \\ X_a^0 \end{bmatrix} = \begin{bmatrix} \mathbf{X}_a^s \\ aX^0 \end{bmatrix} = \begin{bmatrix} X_a^1 \\ \cdot \\ \cdot \\ \cdot \\ X_a^5 \\ aX^0 \end{bmatrix} := X^0 \begin{bmatrix} a_1 s^{11} + a_2 s^{22} \\ a_3 s^{11} + a_4 s^{22} \\ s^{23} \\ s^{13} \\ s^{12} \\ a \end{bmatrix} \tag{84}$$

be an augmented six-dimensional stress vector, and from Eqs. (81) and (83) it follows that

$$\dot{\mathbf{X}}_a = \mathbf{A}_a \mathbf{X}_a, \tag{85}$$

where

$$\mathbf{A}_a := \begin{bmatrix} \mathbf{0}_{5\times 5} & \mathbf{A}_a^s \\ (\mathbf{A}_a^s)^{\mathrm{T}} & 0 \end{bmatrix}, \quad \mathbf{A}_a^s := 2Ga^{-1} \begin{bmatrix} a_1\dot{e}_{11} + a_2\dot{e}_{22} \\ a_3\dot{e}_{11} + a_4\dot{e}_{22} \\ \dot{e}_{23} \\ \dot{e}_{13} \\ \dot{e}_{12} \end{bmatrix}. \tag{86}$$

Similarly, define another integrating factor by

$$x^0 := \exp\left(\frac{-9K\alpha^2\lambda}{\tau_y}\right) = (X^0)^{-9K\alpha^2/G}, \tag{87}$$

and thus Eq. (12) can be written as

$$\frac{\mathrm{d}}{\mathrm{d}t}[x^0(\tau_y - \alpha \mathrm{tr}\,\boldsymbol{\sigma})] = -3K\alpha x^0 \mathrm{tr}\,\dot{\boldsymbol{\varepsilon}}. \tag{88}$$

Taking the product of Eq. (88) with $\tau_y - \alpha \mathrm{tr}\,\boldsymbol{\sigma}$ and noting that $(\tau_y - \alpha \mathrm{tr}\,\boldsymbol{\sigma})\mathrm{d}(\tau_y - \alpha \mathrm{tr}\,\boldsymbol{\sigma})/\mathrm{d}t = b\dot{b}$ and $(\tau_y - \alpha \mathrm{tr}\,\boldsymbol{\sigma})^2 = b^2$ by Eq. $(82)_2$, we obtain

$$\frac{\mathrm{d}}{\mathrm{d}t}(bx^0) = -3K\alpha x^0 b^{-1}(\tau_y - \alpha \mathrm{tr}\,\boldsymbol{\sigma})\mathrm{tr}\,\dot{\boldsymbol{\varepsilon}}. \tag{89}$$

Let

$$\mathbf{X}_b := \begin{bmatrix} X_b^1 \\ X_b^0 \end{bmatrix} = \begin{bmatrix} x^0(\tau_y - \alpha \mathrm{tr}\,\boldsymbol{\sigma}) \\ bx^0 \end{bmatrix}. \tag{90}$$

From Eqs. (88) and (89) we obtain

$$\dot{\mathbf{X}}_b = \mathbf{A}_b \mathbf{X}_b, \tag{91}$$

where

$$\mathbf{A}_b := \begin{bmatrix} 0 & -3K\alpha b^{-1}\mathrm{tr}\,\dot{\boldsymbol{\varepsilon}} \\ -3K\alpha b^{-1}\mathrm{tr}\,\dot{\boldsymbol{\varepsilon}} & 0 \end{bmatrix}. \tag{92}$$

In above derivations we split the yield condition as shown by Eq. $(82)_3$ into two "sub-yield" conditions as shown by Eqs. $(82)_1$ and $(82)_2$, respectively. The former after multiplying by $(X^0)^2$ on both sides can be written as, in terms of $\mathbf{X}_a$ defined by Eq. (84),

$$\mathbf{X}_a^{\mathrm{T}} \mathbf{g}_a \mathbf{X}_a = \|\mathbf{X}_a^s\|^2 - (X_a^0)^2 = (X^0)^2 \left[\frac{1}{2}\|\mathbf{s}\|^2 - a^2\right] = 0, \tag{93}$$

where

$$\mathbf{g}_a = \begin{bmatrix} \mathbf{I}_5 & \mathbf{0}_{5\times 1} \\ \mathbf{0}_{1\times 5} & -1 \end{bmatrix} \tag{94}$$

is an indefinite metric tensor of the six-dimensional Minkowski spacetime $\mathbb{M}^{5+1}$. Eq. (93) corresponds to a cone in the space of $\mathbf{X}_a$ in $\mathbb{M}^{5+1}$. Since $\mathbf{A}_a$ in the dynamical law (85) satisfying

$$\mathbf{A}_a^{\mathrm{T}} \mathbf{g}_a + \mathbf{g}_a \mathbf{A}_a = \mathbf{0} \tag{95}$$

is an (5+1)-dimensional Lie algebra of the proper orthochronous Lorentz group $SO_o(5,1)$, $\mathbf{G}_a$ generated from Eq. (85) satisfies the following group properties:

$$\mathbf{G}_a^{\mathrm{T}}\mathbf{g}_a\mathbf{G}_a = \mathbf{g}_a, \quad \det\mathbf{G}_a = 1, \quad (G_a)_0^0 \geqslant 1, \tag{96}$$

where $(G_a)_0^0$ denotes the zeroth component of $\mathbf{G}_a$.

Correspondingly, Eq. $(82)_2$ after multiplying by $(x^0)^2$ on both sides can be written as, in terms of $\mathbf{X}_b$ defined by Eq. (90),

$$\mathbf{X}_b^{\mathrm{T}}\mathbf{g}_b\mathbf{X}_b = \|\mathbf{X}_b^s\|^2 - (X_b^0)^2 = (x^0)^2[(\tau_y - \alpha\mathrm{tr}\boldsymbol{\sigma})^2 - b^2] = 0, \tag{97}$$

where

$$\mathbf{g}_b = \begin{bmatrix} 1 & 0 \\ 0 & -1 \end{bmatrix}. \tag{98}$$

Eq. (97) corresponds to a cone in the space of $\mathbf{X}_b$ in $\mathbb{M}^{1+1}$. Since $\mathbf{A}_b$ in the dynamical law (91) satisfying

$$\mathbf{A}_b^{\mathrm{T}}\mathbf{g}_b + \mathbf{g}_b\mathbf{A}_b = \mathbf{0} \tag{99}$$

is an (1+1)-dimensional Lie algebra of the proper orthochronous Lorentz group $SO_o(1,1)$, $\mathbf{G}_b$ generated from Eq. (91) satisfies the following group properties:

$$\mathbf{G}_b^{\mathrm{T}}\mathbf{g}_b\mathbf{G}_b = \mathbf{g}_b, \quad \det\mathbf{G}_b = 1, \quad (G_b)_0^0 \geqslant 1. \tag{100}$$

From a geometric view, the underlying space of $\mathbf{X}_a$ and $\mathbf{X}_b$ which governed respectively by Eqs. (85) and (91) together with the two cone conditions (93) and (97) is a direct product of $\mathbb{M}^{5+1} \otimes \mathbb{M}^{1+1}$ as shown in Fig. 4. The internal symmetry group of the above two integrating factors system is $SO_o(5,1) \otimes SO_o(1,1)$.

For calculation purpose we now derive a numerical scheme based on the two integrating factors formulation. The numerical scheme would provide a medium to calculate the values of $\mathbf{X}_a$ and $\mathbf{X}_b$ at time $t = t_{\ell+1}$ when knowing $\mathbf{X}_a$ and $\mathbf{X}_b$ at time $t = t_\ell$.

The evolution of $\mathbf{X}_a$ is governed by the dynamical law (85) with matrix $\mathbf{A}_a$ given by Eq. (86). Due to the piecewise linearity of controlled strain, $\dot{\mathbf{e}}$ is constant in each time increment equal to Δt. Unluckily, due to the presence of $a(t)$ in Eq. (86), this is not true for matrix $\mathbf{A}_a$. Therefore we approximate the solution of the dynamical law (85) by considering a constant in each single time step. Under such an additional hypothesis, the matrix $\mathbf{A}_a$ is constant, and so the numerical solution of Eq. (85) is known to be

$$\mathbf{X}_a(\ell+1) = \mathbf{G}_a(\ell)\mathbf{X}_a(\ell), \tag{101}$$

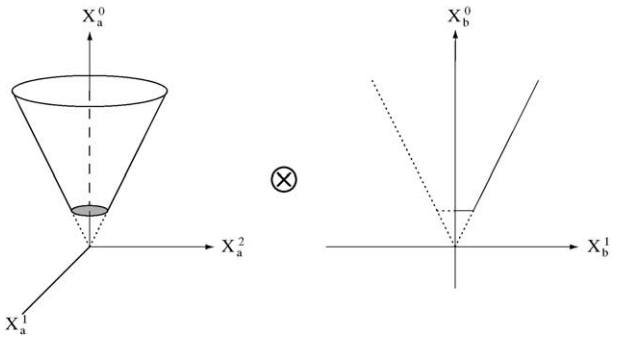

Fig. 4. The Drucker–Prager yield cone is extended to a twin-cone in the product space of $\mathbb{M}^{5+1} \otimes \mathbb{M}^{1+1}$. It is the construction of the twin-cone in Minkowski spacetimes of $\mathbf{X}_a$ and $\mathbf{X}_b$ that signifies a conceptual breakthrough.

where

$$\mathbf{G}_a(\ell) := \exp[\Delta t \mathbf{A}_a(\ell)] = \begin{bmatrix} \mathbf{I}_5 + \frac{(z_3-1)}{\mathbf{A}_a^s(\ell)\cdot\mathbf{A}_a^s(\ell)}\mathbf{A}_a^s(\ell)(\mathbf{A}_a^s)^{\mathrm{T}}(\ell) & \frac{z_4\mathbf{A}_a^s(\ell)}{\sqrt{\mathbf{A}_a^s(\ell)\cdot\mathbf{A}_a^s(\ell)}} \\ \frac{z_4(\mathbf{A}_a^s)^{\mathrm{T}}(\ell)}{\sqrt{\mathbf{A}_a^s(\ell)\cdot\mathbf{A}_a^s(\ell)}} & z_3 \end{bmatrix}, \tag{102}$$

in which

$$z_3 := \cosh\left(\Delta t\sqrt{\mathbf{A}_a^s(\ell)\cdot\mathbf{A}_a^s(\ell)}\right), \quad z_4 := \sinh\left(\Delta t\sqrt{\mathbf{A}_a^s(\ell)\cdot\mathbf{A}_a^s(\ell)}\right). \tag{103}$$

A similar argument applied to the dynamical law (91) with matrix $\mathbf{A}_b$ given by Eq. (92) leads to

$$\mathbf{X}_b(\ell+1) = \mathbf{G}_b(\ell)\mathbf{X}_b(\ell), \tag{104}$$

where

$$\mathbf{G}_b(\ell) := \exp[\Delta t \mathbf{A}_b(\ell)] = \begin{bmatrix} \cosh(-3K\alpha b^{-1}(\ell)\mathrm{tr}\,\dot{\boldsymbol{\varepsilon}}(\ell)\Delta t) & \sinh(-3K\alpha b^{-1}(\ell)\mathrm{tr}\,\dot{\boldsymbol{\varepsilon}}(\ell)\Delta t) \\ \sinh(-3K\alpha b^{-1}(\ell)\mathrm{tr}\,\dot{\boldsymbol{\varepsilon}}(\ell)\Delta t) & \cosh(-3K\alpha b^{-1}(\ell)\mathrm{tr}\,\dot{\boldsymbol{\varepsilon}}(\ell)\Delta t) \end{bmatrix}. \tag{105}$$

However, in their current forms Eqs. (101) and (104) insuffice to determine the values of $\mathbf{s}(\ell+1)$ and $\mathrm{tr}\,\boldsymbol{\sigma}(\ell+1)$, since from Eqs. (84) and (90) we have

$$\begin{bmatrix} s^{11}(\ell+1) \\ s^{22}(\ell+1) \\ s^{23}(\ell+1) \\ s^{13}(\ell+1) \\ s^{12}(\ell+1) \end{bmatrix} = \begin{bmatrix} a_4 & -a_2 & \mathbf{0}_{2\times3} \\ -a_3 & a_1 & \\ \mathbf{0}_{3\times2} & & \frac{\sqrt{3}}{2}\mathbf{I}_3 \end{bmatrix} \frac{2a(\ell+1)}{\sqrt{3}X_a^0(\ell+1)}\mathbf{X}_a^s(\ell+1), \tag{106}$$

$$\mathrm{tr}\,\boldsymbol{\sigma}(\ell+1) = \frac{1}{\alpha}\left[\tau_y - \frac{X_b^1(\ell+1)}{X_b^0(\ell+1)}b(\ell+1)\right], \tag{107}$$

and there are still two unknowns $a(\ell+1)$ and $b(\ell+1)$ on the right-hand sides. For this problem we need four equations:

$$X^0(\ell+1)a(\ell+1) = X_a^0(\ell+1), \tag{108}$$

$$x^0(\ell+1)b(\ell+1) = X_b^0(\ell+1), \tag{109}$$

$$a^2(\ell+1) - b^2(\ell+1) = 0, \tag{110}$$

$$x^0(\ell+1) - (X^0(\ell+1))^{-9K\alpha^2/G} = 0, \tag{111}$$

to solve four unknowns $a(\ell+1)$, $b(\ell+1)$, $X^0(\ell+1)$ and $x^0(\ell+1)$. In above the values on right-hand sides are all known. Eq. (108) is obtained from the last row in Eq. (84); Eq. (109) is obtained from the last row in Eq. (90); Eq. (110) is a direct result of Eq. $(82)_3$; and Eq. (111) is obtained from Eq. (87). Through some algebraic manipulations we obtain the solution of $X^0(\ell+1)$ by

$$X^0(\ell+1) = \left(\frac{X_a^0(\ell+1)}{X_b^0(\ell+1)}\right)^{G/R}, \tag{112}$$

and $a(\ell+1)$ can be calculated by Eq. (108). Then $x^0(\ell+1)$ is calculated by Eq. (111), and $b(\ell+1)$ can be obtained from Eq. (109). Substituting $a(\ell+1)$ and $b(\ell+1)$ into Eqs. (106) and (107) we thus obtain $\mathbf{s}(\ell+1)$ and $\mathrm{tr}\,\boldsymbol{\sigma}(\ell+1)$.

Especially, we have forcing the consistency condition by Eq. (110), and so the new scheme not only preserves the cone conditions

$$\mathbf{X}_a^{\mathrm{T}}(\ell+1)\mathbf{g}_a\mathbf{X}_a(\ell+1)=0,\quad \mathbf{X}_b^{\mathrm{T}}(\ell+1)\mathbf{g}_b\mathbf{X}_b(\ell+1)=0, \tag{113}$$

but also the consistency condition

$$\frac{1}{2}\|\mathbf{s}(\ell+1)\|^2-[\tau_y-\alpha\mathrm{tr}\boldsymbol{\sigma}(\ell+1)]^2=0. \tag{114}$$

The equality in Eq. (114) says nothing but for every time increment the stress point $\boldsymbol{\sigma}(\ell+1)$ is located on the yield hyper-surface. In other words, the consistency condition is fulfilled exactly for every time step in the on-phase. Therefore, the new numerical scheme may be specifically called a consistent scheme. This explains why this scheme provides a zero error of the consistency condition as shown in Fig. 3.

10. Runge–Kutta scheme based on integral constitutive solution

In terms of

$$\dot{\Lambda}:=\frac{\tau_y-\alpha\mathrm{tr}\boldsymbol{\sigma}}{\tau_y}\dot{\lambda}, \tag{115}$$

Eqs. (12) and (13) can be written as

$$\mathrm{tr}\dot{\boldsymbol{\sigma}}=3K\mathrm{tr}\dot{\boldsymbol{\varepsilon}}-9K\alpha\dot{\Lambda}, \tag{116}$$

$$\dot{\mathbf{s}}=2G\dot{\mathbf{e}}-\frac{G\dot{\Lambda}}{\tau_y-\alpha\mathrm{tr}\boldsymbol{\sigma}}\mathbf{s}. \tag{117}$$

The integrals of the above two equations are

$$\mathrm{tr}\boldsymbol{\sigma}(t)=\mathrm{tr}\boldsymbol{\sigma}(\tau)+3K\Delta\mathrm{tr}\boldsymbol{\varepsilon}-9K\alpha[\Lambda(t)-\Lambda(\tau)], \tag{118}$$

$$\mathbf{s}(t)=\frac{1}{Y(\Lambda(t))}\left[Y(\Lambda(\tau))\mathbf{s}(\tau)+\int_\tau^t 2GY(\Lambda(\xi))\dot{\mathbf{e}}(\xi)\,\mathrm{d}\xi\right], \tag{119}$$

where $\Delta\mathrm{tr}\boldsymbol{\varepsilon}$ is a constant volumetric strain increment at each time step increment $\Delta t=t-\tau$, and Y is defined by

$$Y(\Lambda):=\exp\left[\int_0^\Lambda\frac{G}{\tau_y-\alpha\mathrm{tr}\boldsymbol{\sigma}(p)}\mathrm{d}p\right]=\left(\frac{c_0+9K\alpha^2\Lambda}{c_0}\right)^{G/(9K\alpha^2)}, \tag{120}$$

where p is a dummy variable to denote Λ, and

$$c_0:=\tau_y-\alpha\mathrm{tr}\boldsymbol{\sigma}(\tau)-3K\alpha\Delta\mathrm{tr}\boldsymbol{\varepsilon}-9K\alpha^2\Lambda(\tau) \tag{121}$$

is a constant.

From Eq. (7) at the yield state we have

$$\frac{1}{2}\mathbf{s}\cdot\mathbf{s}=(\tau_y-\alpha\mathrm{tr}\boldsymbol{\sigma})^2, \tag{122}$$

$$\frac{1}{2}\mathbf{s}\cdot\dot{\mathbf{s}}=-\alpha(\tau_y-\alpha\mathrm{tr}\boldsymbol{\sigma})\mathrm{tr}\dot{\boldsymbol{\sigma}}. \tag{123}$$

Inserting Eq. (116) for $\mathrm{tr}\,\dot{\boldsymbol{\sigma}}$ and Eq. (117) for $\dot{\mathbf{s}}$ into Eq. (123) and considering Eq. (122), we obtain

$$(\tau_y - \alpha \mathrm{tr}\,\boldsymbol{\sigma})(R\dot{\Lambda} - 3K\alpha \mathrm{tr}\,\dot{\boldsymbol{\varepsilon}}) = G\mathbf{s}\cdot\dot{\mathbf{e}}, \tag{124}$$

where R was defined by Eq. (21). Taking the time derivative of Eq. (124) while keeping $\dot{\mathbf{e}}$ and $\mathrm{tr}\,\dot{\boldsymbol{\varepsilon}}$ to be constant, inserting Eqs. (116) and (117) and then combining with Eq. (124) again, yield

$$(c_0 + 9K\alpha^2\Lambda)R\ddot{\Lambda} - 6K\alpha R\,\mathrm{tr}\,\dot{\boldsymbol{\varepsilon}}\dot{\Lambda} + R^2\dot{\Lambda}^2 = 2G^2\|\dot{\mathbf{e}}\|^2 - 9K^2\alpha^2(\mathrm{tr}\,\dot{\boldsymbol{\varepsilon}})^2. \tag{125}$$

The above is a second order autonomous differential equation for Λ. Any desired degree of accuracy can be achieved by employing high-order Runge–Kutta methods to integrate Eq. (125). In the calculations presented in Fig. 3 the above equation was integrated by a fourth-order Runge–Kutta method, which together with the discretization of Eq. (119) by the trapezoidal rule

$$\mathbf{s}(t) = \frac{Y(\Lambda(\tau))}{Y(\Lambda(t))}\mathbf{s}(\tau) + G\Delta t\left[1 + \frac{Y(\Lambda(\tau))}{Y(\Lambda(t))}\right]\dot{\mathbf{e}}(\tau), \tag{126}$$

and Eq. (118) provide a numerical method to calculate the stress. We call it the Runge–Kutta scheme. The result of consistency error is shown in Fig. 3, the values of which may be large to 5 (psi)^2.

In order to enhance the accuracy of consistency we may substitute Eqs. (118) and (126) into the yield condition (122) to obtain a non-linear algebraic equation for Λ:

$$\begin{aligned} &Y^2(\Lambda(\tau))\mathbf{s}(\tau)\cdot\mathbf{s}(\tau) + 2G\Delta t\mathbf{s}(\tau)\cdot\dot{\mathbf{e}}(\tau)Y(\Lambda(\tau))[Y(\Lambda(t)) + Y(\Lambda(\tau))] + (G\Delta t)^2\|\dot{\mathbf{e}}(\tau)\|^2[Y(\Lambda(t)) \\ &\quad + Y(\Lambda(\tau))]^2 - 2[c_0 + 9K\alpha^2\Lambda(t)]^2Y^2(\Lambda(t)) \\ &\quad = 0. \end{aligned} \tag{127}$$

Solving this equation by the Newton–Raphson method with error tolerance 10^{-8}, and using Eqs. (118) and (126) to calculate the stress, the result of consistency error is shown in Fig. 3 marked by the Newton–Raphson scheme, which largely improves the accuracy to the order of 10^{-10}. As compared to the consistent schemes developed in Sections 8 and 9, this scheme spends much time on the iterative solution of the above equation. As compared with the Runge–Kutta scheme the errors of the above three schemes are almost zero as shown in Fig. 3.

Because the one-integrating factor scheme and the two-integrating factors scheme automatically match the consistency condition without any iteration, they can save about 90% or more CPU time than the backward Euler integration scheme (Simo and Hughes, 1998). For example, the computational time of the new schemes spent in the computation of the above numerical example in Fig. 2 is about 0.2 s, but the backward Euler integration scheme requires 2 s.

11. Conclusions

In this paper we have investigated the internal symmetry inherent in a constitutive model of Drucker–Prager type. Even though the constitutive equations are highly non-linear in the stress space of $\boldsymbol{\sigma}$, they can be converted to a Lie type system $\dot{\mathbf{X}} = \mathbf{AX}$ in the seven-dimensional augmented stress space of $\mathbf{X}$. In the augmented stress space an internal spacetime structure of the pseudo-Riemannian type is brought out. The control tensor $\mathbf{A}$ for the plastic phase was proved to be an element of the real Lie algebra $sl(5,2,\mathbb{R})$ of the special orthochronous pseudo-linear group $SL(5,2,\mathbb{R})$, and the one-parameter subgroup $\mathbf{G}$ of the system $\dot{\mathbf{G}} = \mathbf{AG}$ with the on-phase $\mathbf{A}$ was shown to be an element of the special orthochronous pseudo-linear group, so that the causality relation of the augmented stresses was verified. To account for both the on and off phases we constructed a composite space endowed with a pseudo-Riemann metric with signature (5,2) on the pseudo-sphere but with a pseudo-Euclidean metric having signature (5,1) on each of the interior

of the cones inside the pseudo-sphere. As a result we found that the Drucker–Prager elastoplastic model possesses two kinds of symmetry—$T(6)$ in the off-phase and $PSL(5,2,\mathbb{R})$ in the plastic phase—and has symmetry switching between the two depending on the control input.

In addition that we also proposed a two-integrating factors formulation of the Drucker–Prager constitutive equations, which splits the yield criterion into two sub-yield functions in deviatoric and volumetric stress spaces. Then, two Lie type differential equations $\dot{\mathbf{X}}_a = \mathbf{A}_a\mathbf{X}_a$ and $\dot{\mathbf{X}}_b = \mathbf{A}_b\mathbf{X}_b$ were constructed. The augmented states $\mathbf{X}_a$ and $\mathbf{X}_b$ satisfy the cone conditions in spaces $\mathbb{M}^{5+1}$ and $\mathbb{M}^{1+1}$, respectively. The Lie algebras are the direct sum of $so(5,1) \oplus so(1,1)$ and the corresponding Lie symmetries are $SO_o(5,1) \otimes SO_o(1,1)$.

Based on these symmetry studies, numerical schemes which preserve the group properties for every time increment were developed. These group preserving schemes may be specifically called consistent schemes, since they are capable, among other benefits derivable from the group properties, of updating the stress point to be automatically located on the yield surface at the end of each time increment in the plastic phase without any iterative calculations, that is, the consistency condition is fulfilled automatically and exactly. In this regard, the conventional numerical schemes typically do not share the group properties so that perform less accurate than the consistent schemes.

Acknowledgements

The financial support provided by the National Science Council under the Grant NSC 92-2212-E-019-006 is gratefully acknowledged.

References

Auricchio, F., Beirão da Veiga, L.B., 2003. On a new integration scheme for von-Mises plasticity with linear hardening. Int. J. Numer. Meth. Eng. 56, 1375–1396.

Borja, R.I., 2000. A finite element model for strain localization analysis of strongly discontinuous fields based on standard Galerkin approximation. Comput. Meth. Appl. Mech. Eng. 190, 1529–1549.

Borja, R.I., Regueiro, R.A., 2001. Strain localization in frictional materials exhibiting displacement jumps. Comput. Meth. Appl. Mech. Eng. 190, 2555–2580.

Bousshine, L., Chaaba, A., De Saxcé, G., 2001. Softening in stress–strain curve for Drucker–Prager non-associated plasticity. Int. J. Plasticity 17, 21–46.

Büttner, J., Simeon, B., 2002. Runge–Kutta methods in elastoplasticity. Appl. Numer. Math. 41, 443–458.

Cocchetti, G., Perego, U., 2003. A rigorous bound on error in backward-difference elastoplastic time-integration. Comput. Meth. Appl. Mech. Eng. 192, 4909–4927.

Drucker, D.C., Prager, W., 1952. Soil mechanics and plastic analysis or limit design. Quart. Appl. Math. 10, 157–165.

Hjiaj, M., Fortin, J., De Saxcé, G., 2003. A complete stress update algorithm for the non-associated Drucker–Prager model including treatment of the apex. Int. J. Eng. Sci. 41, 1109–1143.

Hong, H.-K., Liou, J.-K., 1993. Integral-equation representations of flow elastoplasticity derived from rate-equation models. Acta Mech. 96, 181–202.

Hong, H.-K., Liu, C.-S., 1999a. Lorentz group $SO_o(5,1)$ for perfect elastoplasticity with large deformation and a consistency numerical scheme. Int. J. Non-linear Mech. 34, 1113–1130.

Hong, H.-K., Liu, C.-S., 1999b. Internal symmetry in bilinear elastoplasticity. Int. J. Non-linear Mech. 34, 279–288.

Hong, H.-K., Liu, C.-S., 2000. Internal symmetry in the constitutive model of perfect elastoplasticity. Int. J. Non-linear Mech. 35, 447–466.

Hughes, T.J.R., 1984. Numerical implementation of constitutive models: rate-independent deviatoric plasticity. In: Nemat-Nasser, S., Asaro, R.J., Hegemier, G.A. (Eds.), Theoretical Foundation for Large-scale Computations of Nonlinear Material Behavior. Martinus Nijhoff Publishers, Dordrecht, pp. 29–63. Chapter 2.

Li, F.Z., Pan, J., 1990. Plane-strain crack-tip fields for pressure-sensitive dilatant materials. J. Appl. Mech. ASME 57, 40–49.

Liu, C.-S., 2001a. The g-based Jordan algebra and Lie algebra with application to the model of visco-elastoplasticity. J. Marine Sci. Technol. 9, 1–13.
Liu, C.-S., 2001b. Cone of non-linear dynamical system and group preserving schemes. Int. J. Non-linear Mech. 36, 1047–1068.
Liu, C.-S., 2003. Symmetry groups and the pseudo-Riemann spacetimes for mixed-hardening elastoplasticity. Int. J. Solids Struct. 40, 251–269.
Liu, C.-S., 2004a. A consistent numerical scheme for the von Mises mixed-hardening constitutive equations. Int. J. Plasticity 20, 663–704.
Liu, C.-S., 2004b. Lie symmetries of finite strain elastic–perfectly plastic models and exactly consistent schemes for numerical integrations. Int. J. Solids Struct. 41, 1823–1853.
Liu, C.-S., Hong, H.-K., 2001. Using comparison theorem to compare corotational stress rates in the model of perfect elastoplasticity. Int. J. Solids Struct. 38, 2969–2987.
Loret, B., Prevost, J.H., 1986. Accurate numerical solutions for Drucker–Prager elastic–plastic models. Comput. Meth. Appl. Mech. Eng. 54, 259–277.
Miao, Y., Drugan, W.J., 1993. Influence of porosity on plane-strain crack-tip stress fields in elastic–plastic materials. J. Appl. Mech. ASME 60, 883–889.
Mukherjee, S., Liu, C.-S., 2003. Computational isotropic-workhardening rate-independent elastoplasticity. J. Appl. Mech. ASME 70, 644–648.
Nagtegaal, J.C., Parks, D.M., Rice, J.R., 1974. On numerically accurate finite element solutions in the fully plastic range. Comput. Meth. Appl. Mech. Eng. 4, 153–177.
Ortiz, M., Popov, E.P., 1985. Accuracy and stability of integration algorithms for elastoplastic constitutive relations. Int. J. Numer. Meth. Eng. 21, 1561–1576.
Simo, J.C., Taylor, R.L., 1985. Consistent tangent operators for rate-independent elastoplasticity. Comput. Meth. Appl. Mech. Eng. 48, 101–118.
Simo, J.C., Hughes, T.J.R., 1998. Computational Inelasticity. Springer, New York.
Wells, G.N., Sluys, L.J., 2001. Analysis of slip planes in three-dimensional solids. Comput. Meth. Appl. Mech. Eng. 190, 3591–3606.